Chapter 3

Generating finite element models of the knee: how accurate can we determine ligament attachment sites from MRI scans?

H.H. Rachmat [1,3,6], D. Janssen [3], W.J. Zevenbergen [3], G.J. Verkerke [4,5], R.L. Diercks [2], N. Verdonschot [3,4]

[1] Department of Biomedical Engineering, University of Groningen, University Medical Center Groningen, A. Deusinglaan 1, 9713 AV Groningen, The Netherlands
[2] Department of Orthopaedics, University of Groningen, University Medical Center Groningen, The Netherlands
[3] Orthopaedic Research Laboratory, Radboud University Nijmegen Medical Centre, P.O. Box 9101, 6500 HB Nijmegen, The Netherlands
[4] Department of Biomechanical Engineering, University of Twente, Enschede, The Netherlands
[5] Department of Rehabilitation Medicine, University of Groningen, University Medical Center Groningen, The Netherlands
[6] Department of Electrical Engineering, Institut Teknologi Nasional (ITENAS) Bandung, West Java, Indonesia.

Journal of Medical Engineering & Physics, 2014, Volume 36, Issue 6; pp. 701-7

Abstract

In this study, we evaluated the intra- and inter- observer variability when determining the insertion and origin sites of knee ligaments on MRI scan images. We collected data of five observers with different backgrounds, who determined the ligament attachment sites in an MRI scan of a right knee of a 66-year-old male cadaver donor. We evaluated the intra- and inter-observer differences between the ligament attachment center points, and also determined the differences relative to a physical measurement performed on the same cadaver. The largest mean intra- and inter-observer differences were 4.30mm (ACL origin) and 16.81mm (superficial MCL insertion), respectively. Relative to the physical measurement, the largest intra- and inter-observer differences were 31.84mm (superficial MCL insertion) and 23.39mm (deep MCL insertion), respectively. The results indicate that, dependent on the location, a significant variation can occur when identifying the attachment site of the knee ligaments. This finding is of particular importance when creating computational models based on MRI data, as the variations in attachment sites may have a considerable effect on the biomechanical behavior of the human knee joint.

Keywords:

Attachment sites, knee, ligament, MRI scan, variability.

1. Introduction

Finite element (FE) models of the knee joint are useful for analyzing knee joint kinematics. They provide insights into the influence of mechanical properties of biological tissues on the performance of structures, reducing both cost and time (Burns et al., 1995). The models are usually based on magnetic resonance imaging (MRI) or computerized tomography (CT) imaging, which are used to develop 3D models of the soft and hard tissues, respectively (Li et al., 1999; Peña et al., 2006; Potočnik et al., 2008; Suggs et al. 2003). The bones of the knee joint can also be constructed using MRI data, only, which has the main advantage that it does not involve ionizing radiation (Li et al., 1999; Suggs et al., 2003; Rathnayaka et al., 2012).

For proper dynamic functioning of the models, it is very important to determine the exact location of ligament attachment sites. The ligaments are segmented from the MRI scans, during which the attachment sites need to be determined. Determining the precise locations for the attachment sites based on MRI is, however, affected by the scan quality and resolution, but also by the inhomogeneous soft tissue conditions, and the level of knowledge of the anatomy of the knee.

The purpose of this study was to evaluate the intra- and inter-observer variability when determining knee ligaments attachment sites based on MRI scans from a cadaveric specimen. These results were then compared with actual physical cadaver measurements.

2. Materials and methods

2.1. MRI-based measurements

The knee ligament attachment sites were measured in a right knee from a 66-year-old male cadaver donor, which was obtained from the Anatomy Department of the Radboud University Medical Center (Nijmegen, The Netherlands). The knee was scanned in a 3-Tesla MRI scan (Siemens, Trim Trio, Erlangen, Germany), using an extremity knee coil. The images were acquired according the following parameters: spin echo scanning sequence with a repetition time of 1200ms, echo time of 29ms, field of view of 224mm x 224mm, matrix size of 448 x 448, pixel size of 0.5mm x 0.5mm and a slice thickness of 0.5 mm, with a total of 240 MRI slices. The dicom files were imported in Mimics 14.0 (Materialise, Leuven, Belgium), which was used to segment the bones (femur, tibia and fibula) into 3D surface models (Figure 1).

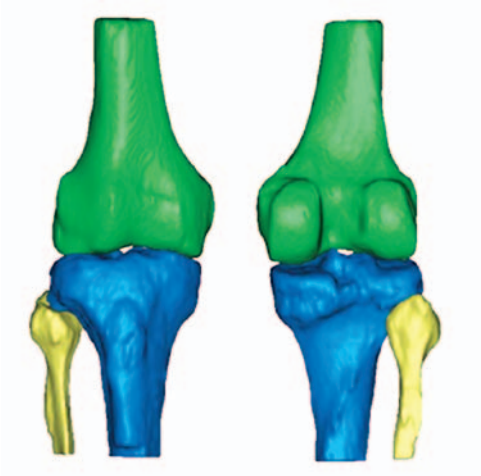

Figure 1. MRI-based 3D surface mesh (anterior (left) and posterior (right) views), consisting of the femur, tibia and fibula.

The following ligament attachment sites were determined on the tibia, femur and fibula: insertion and origin of the anterior cruciate ligament (ACL-tibia and ACL-femur), insertion and origin of the posterior cruciate ligament (PCL-tibia and PCL-femur), insertion and origin of the lateral collateral ligament (LCL-fibula and LCL-femur) as well as two insertions and the origin of the superficial and deep medial collateral ligament (SMCL-tibia, DMCL-tibia and MCL-femur).

Five observers participated in this study; an orthopaedic surgeon (TvT), an engineering PhD student (HR), an engineering PostDoc (PT) and two resident medical doctors (LN and JS). One observer (HR) conducted all observations three times with a minimum interval of one week for evaluating the intra-observer reliability. A protocol for the ligament attachment site measurements, guidelines for using the software to mark the sites, and an anatomical atlas were provided for the observers during the measurements. All observers independently determined the attachment sites, using

Mimics 14.0. Using this program, the observers manually marked the attachment sites on the MRI scan (Figure 2). The observers had all three orthogonal planes available to inform them on the attachment site position, but they were free in the choice of the planes in which they indicated the ligament attachment site.

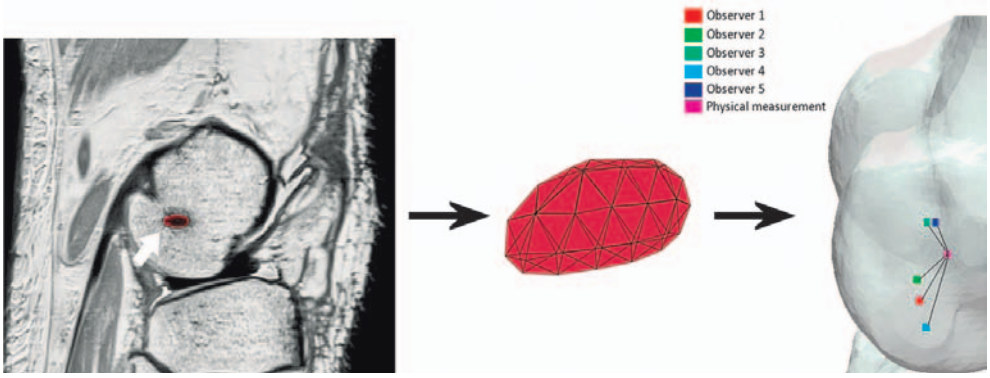

Figure 2. For the determination of the MRI-based measurements, first the attachment site was marked on the MRI-image, using Mimics 14.0 (left). Next the region was converted to a 3D triangular surface (center, magnified). Based on this triangular surface, the center point of the attachment site was calculated, and compared with the physical measurement (right).

After the observations were performed, all marked attachment sites were converted into 3D triangular surfaces in Mimics 14.0, and exported in STL-format. The surface models of the bones were used for the comparison between observers, and between the MRI-based measurements and the physical measurements. Therefore, all exported attachment sites as indicated by the observers were projected onto the bone surfaces in Matlab R2011 (The MathWorks, Natick, Massachusetts, USA), using the iterative closest point (ICP) method (Besl and McKay, 1992). The ICP method is an iterative descent procedure, which seeks to minimize the sum of square distances between all points from the MRI-based measurement and their closest points in the bone surface models. In order to project the MRI-based measurements onto the bone surfaces, the measured points were translated over a mean distance of 1.15 ± 1.13mm for the femoral, and 0.86 ± 0.70 mm for the tibial attachment sites.

The centroid of the projected area was then determined by dividing the area into triangular parts with the same normal direction. For each triangular part, the geometric center and area were calculated. The geometric center of the complete area, giving the attachment site, was then defined as the average of all geometric centers, weighted for the area of each triangular part. The centroid for each marking area was then further processed using Matlab R2011 (The MathWorks, Natick, Massachusetts, USA) to quantify the intra- and inter-observer variability, and to compare the MRI-based measurements with the physical measurements (see section 2.3).

2.2. Physical cadaver measurement

In order perform the physical measurements, the knee was dissected by an experienced orthopaedic surgeon (RD), who measured the attachment sites of the ligaments using an electromagnetic tracking system (3Space Fastrak, Polhemus Incorporated, Vermont, USA). The accuracy of the electromagnetic system is 0.8mm and 0.15°, with a resolution of 0.20mm and 0.025° (3Space user's manual, Polhemus Incorporated, Vermont, USA). For each ligament, first, an attachment site was identified and marked by the surgeon. The ligament was then separated from the bone, after which the attachment site was digitized using the stylus.

Before performing the measurement, two reference frames with electromagnetic sensors were placed onto the femur and tibia. An electromagnetic sensor-based stylus was used to measure 3D points relative to the corresponding reference frame. For registration purposes, also points of the femur, tibia and fibula surfaces were collected (Figure 3). These points were used to register the physical measurements to the STL-files of the bone surfaces, previously obtained from the MRI scans.

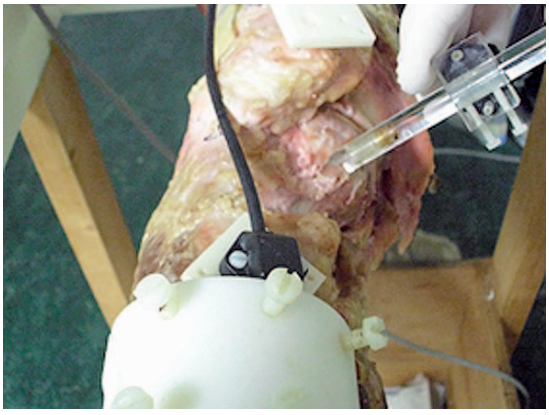

Figure 3. Collecting registration points using an electromagnetic Fastrak sensor-based stylus of three bony surfaces.

For the registration of the physical measurements onto the 3D surface model of the bone, again the ICP method was used. These physical values were used as reference values for comparison with the points measurement from MRI observations.

2.3. Data processing

To quantify the intra- and inter-observer variability, we calculated the distances between measurements relative to two different reference points. For each attachment site, reference point one was the mean of all observations of the MRI observers (intra-observer and inter-observer) (Victor et al., 2009), serving as a reference for the analysis of the accuracy and precision of MRI-based measurements. Reference point two was the position of the physical cadaver measurement $R(x_R, y_R, z_R)$, serving as a

reference to analyze the validity of MRI-based measurements. The mean intra-observer ($P(x_P, y_P, z_P)$) and inter-observer ($Q(x_Q, y_Q, z_Q)$) points were calculated as follows:

$$P(x_P, y_P, z_P) = \frac{P_1+P_2+P_3}{3} \rightarrow \begin{matrix} x_P = \frac{x_{P1}+x_{P2}+x_{P3}}{3} \\ y_P = \frac{y_{P1}+y_{P2}+y_{P3}}{3} \\ z_P = \frac{z_{P1}+z_{P2}+z_{P3}}{3} \end{matrix} \quad [1]$$

$$Q(x_Q, y_Q, z_Q) = \frac{Q_1+Q_2+Q_3+Q_4+Q_5}{5} \rightarrow \begin{matrix} x_Q = \frac{x_{Q1}+x_{Q2}+x_{Q3}+x_{Q4}+x_{Q5}}{5} \\ y_Q = \frac{y_{Q1}+y_{Q2}+y_{Q3}+y_{Q4}+y_{Q5}}{5} \\ z_Q = \frac{z_{Q1}+z_{Q2}+z_{Q3}+z_{Q4}+z_{Q5}}{5} \end{matrix} \quad [2]$$

To quantify the intra(A)-observer accuracy (Figure 4), the distance between the individual observer position relative to the mean position (P) of intra-observers (D_{APPi}), and relative to the point position (R) of the cadaver measurements (D_{ARPi}) were calculated as follows:

$$D_{APPi} = \|P - P_i\| = \sqrt{(x_P - x_{Pi})^2 + (y_P - y_{Pi})^2 + (z_P - z_{Pi})^2} \quad [3]$$

$$D_{ARPi} = \|R - P_i\| = \sqrt{(x_R - x_{Pi})^2 + (y_R - y_{Pi})^2 + (z_R - z_{Pi})^2} \quad [4]$$

The inter(E)-observer accuracy (Figure 4) was also determined by calculating the distance between the individual observer points relative to the mean position (Q) of all observers (D_{EQQj}), and relative to the position (R) of the cadaver measurements (D_{ERQj}):

$$D_{EQQj} = \|Q - Q_j\| = \sqrt{(x_Q - x_{Qj})^2 + (y_Q - y_{Qj})^2 + (z_Q - z_{Qj})^2} \quad [5]$$

$$D_{ERQj} = \|R - Q_j\| = \sqrt{(x_R - x_{Qj})^2 + (y_R - y_{Qj})^2 + (z_R - z_{Qj})^2} \quad [6]$$

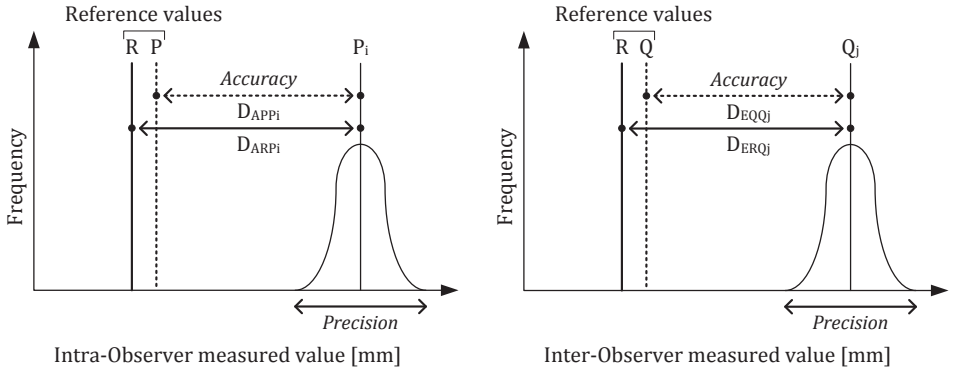

Figure 4. Accuracy and precision quantification of the intra(A)-observer (P_i) and inter(E)-observer (Q_j) relative to the mean observed point (P and Q) and cadaver measurement point (R).

The subscript P refers to the mean intra-observer point position, Q refers to the mean inter-observer point position, R refers to the mean position of the physical measurement, i refers to the 3 intra-observer measurements, and j refers to the 5 inter-observer measurements.

We then calculated the maximum and mean value, and the standard deviation (precision values) of the distance (D_{APPi} , D_{ARPi} , D_{EQQj} , D_{ERQj}) for each ligament location as a measure of the overall intra-observer and inter-observer variability.

3. Results

Compared to the mean MRI-based measurements, the mean intra-observer accuracy ranged from 0.31 mm (LCL origin) to 4.30 mm (ACL origin) (Figure 5). Compared to the physical measurement, the mean intra-observer accuracy ranged from 4.12 mm (MCL origin) to 31.84 mm (SMCL origin) (Figure 6). For all knee ligament attachment sites, the differences were smaller when compared to the mean MRI-based measurements, than when compared to the physical measurements. The intra-observer precision of the measurements was the highest for the femoral attachment site of the lateral collateral ligament (0.17 mm), while it was the lowest for the femoral attachment of the anterior cruciate ligament (4.10 mm).

The mean inter-observers accuracy ranged from 2.43 mm (MCL origin) to 16.81 mm (SMCL insertion) when compared to the MRI-based measurements (Figure 7), whereas relative to the physical measurements, the mean accuracy ranged from 4.99 mm (MCL origin) to 23.39 mm (DMCL insertion) (Figure 8). Similar to the intra-observer accuracy, for all knee ligament attachment sites, the inter-observer differences were smaller when compared to the mean MRI-based measurements, than when compared to the physical measurements. The inter-observer precision was the highest for the femoral attachment site of the medial collateral ligament (0.65 mm), while it was the lowest for the tibial attachment site of the superficial medial collateral ligament (13.47 mm).

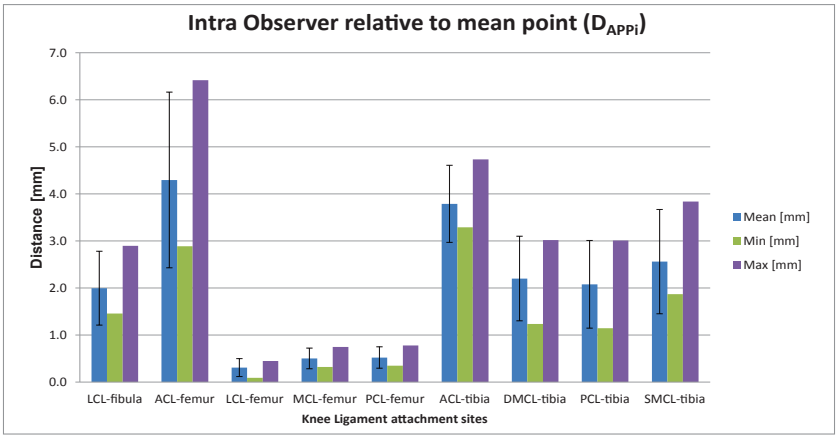

Figure 5. Variability in distance of the ligament attachment sites relative to the mean observed position for the intra-observer comparison.

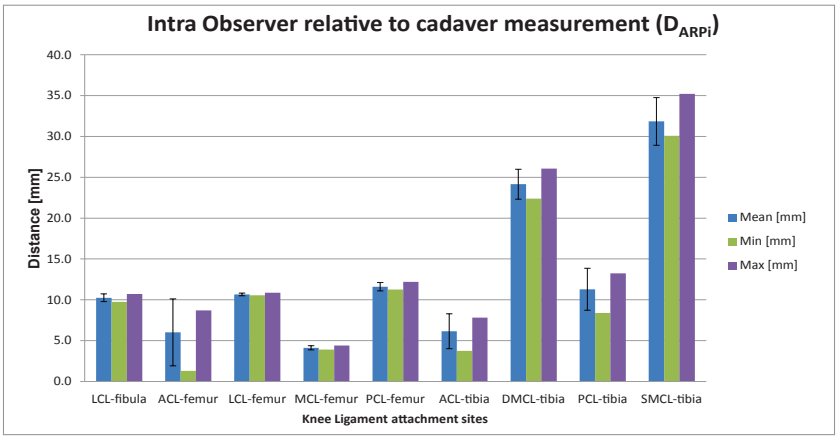

Figure 6. Variability in distance of the ligament attachment sites relative to the position of the physical cadaver measurements for the intra-observer comparison.

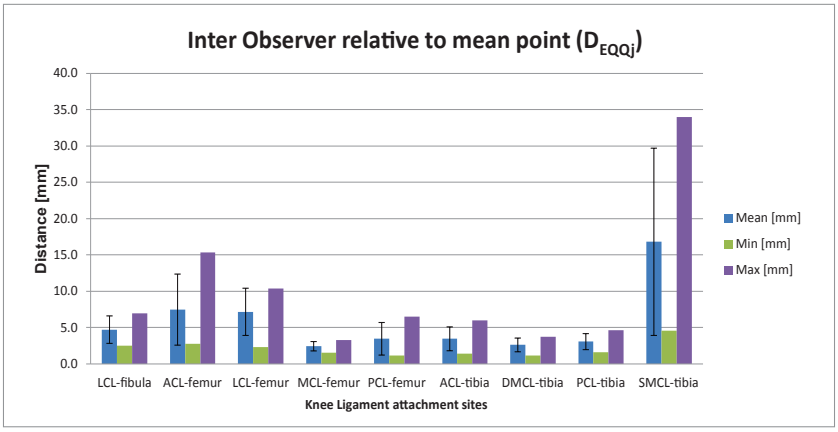

Figure 7. Variability in distance of the ligament attachment sites relative to the mean observed position for the inter-observer comparison.

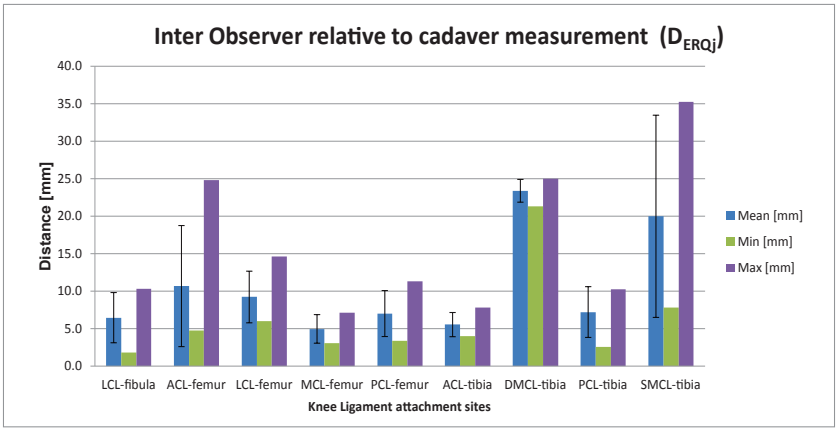

Figure 8. Variability in distance of the ligament attachment sites relative to the position of the physical cadaver measurements for the inter observer comparison.

4. Discussion

The purpose of this study was to evaluate the intra- and inter-observer variability when determining knee ligaments attachment sites based on MRI scans, as this variability may have a considerable effect on the biomechanical behavior of computational models.

Dependent on the specific structure, this study demonstrated that most attachment sites could be determined from MRI within a range from 5-10mm. However, some ligament attachment sites, such as the deep and superficial MCL insertion, are more difficult to replicate, with an average error of up to 23.39mm. This difference could be due to the choice of the MRI plane of view in which the observer determined the attachment site, although the observers had all three planes available. Moreover, the resolution of the MRI-scan (0.5x0.5mm resolution, with a 0.5mm slice thickness) does not explain errors of this magnitude. Most likely, the contrast of the ligament attachment sites with respect to the surrounding hard and soft tissues is the limiting factor. Another source of error is the fact that the attachment sites, which typically comprise a larger area, were reduced to single points in our measurements. This could be the case particularly for the superficial MCL, which has an attachment area of up to 348.6 ± 42.8 mm^2 (Liu et al., 2010). This evidently increases the room for error when compared to ligaments with a smaller, better defined attachment site. Interestingly, for the deep MCL, the intra- and inter-observer accuracy and precision (expressed as the standard deviation) were quite similar (24.16 ±1.83mm and 23.39 ± 1.51mm, respectively). The fact that the variability within and between observers are similar further emphasizes the complexity of identifying this structure on MRI images.

The limitations to the current study are the limited number of observers (n=5), and the limited number of repetitions (n=3) for determining the intra-observer accuracy and precision. The accuracy and precision considerably depended on the particular attachment that was measured. The comparison with physical measurements was performed only by one observer. However, this observer is a senior orthopaedic surgeon, with ample experience in ligament reconstructive surgery.

This study is aimed at identifying the errors that are made when creating computational models of the human knee. Such models give the possibility to analyze the changes that occur in knee kinematics and biomechanics when varying the attachment sites of the knee ligaments. As such, they can inform orthopaedic surgeons on surgical strategies, provided that the models are exact in their representation of the anatomy. If the modeling errors are in the same range as the surgical errors, it will be difficult to model surgical variations in a valid manner.

An inappropriate choice of location of ligament attachment site affects the success of the reconstruction, dependent on the particular ligament. Several studies have shown that defining the appropriate tunnel location during ligament reconstruction is one of the key factors to reconstruct normal knee kinematics. Bedi et al. (Bedi et al., 2010) and Howell (Howell, 1998) showed that a proper orientation of the tibial ACL tunnel results in favorable knee kinematics, reducing complications such as graft impingement

and anterior knee pain. Likewise, the study of Zavras et al. (Zavras et al., 2005) reported that in ACL reconstructions, a small change of 3 mm in the femoral attachment site has a large effect on laxity and tension patterns.

In the case of PCL reconstructions, a proper femoral attachment site has been shown to significantly improve joint stability (Galloway et al., 1996), but it also affects the knee kinematics (Petersen et al., 2006), the graft force (Oakes et al., 2003) and graft tension (Mannor et al., 2000; Shearn et al., 2004). Burns et al. (Burns et al., 1995) stated specifically that placing the femoral tunnel 5 mm proximally and distally to the isometric point results in a decrease and increase in graft tension with knee flexion, respectively. The tibial attachment site, however, produces only minor changes in magnitude of posterior tibial translation (Galloway et al., 1996) and has a smaller effect on graft tension (Burns et al., 1995).

For MCL reconstructions, the relocation of the ligament in the femoral attachment site has an effect on the length of the ligament, which influences the tightness of the ligament during knee flexion (Bartel et al., 1977). The same study also reported that the tibial attachment sites is not critical to the knee-flexion angle. Meister et al. (Meister et al., 2000) reported that the error in the determination of an appropriate LCL attachment site in the femoral bone could result in a disruption of the normal dynamics of knee motion, initiating premature arthritic changes.

These examples show that the magnitude of errors found in this study are too large to generate a reliable cadaver-specific biomechanical model. Apart from the insertion sites, the length of the ligaments (and therewith the slack-length) is also important to determine. We believe that determining this from MRI scans is even more challenging than the determination of the insertion sites. Automated (full or semi) segmentation of the soft tissues (Baldwin et al., 2010; Swanson et al., 2010), perhaps in combination with probabilistic modeling techniques (Bryan et al., 2009; Bryan et al., 2010; Fitzpatrick et al., 2011; Galloway et al., 2012) could assist in generating subject-specific models in a more reliable fashion. Although these techniques work well for bony structures (Rathnayaka et al., 2012; Liu et al., 2010), it yet needs to be confirmed that these techniques will lead to a truly subject-specific representation of the soft tissues as well.

5. Conclusions

The current study demonstrates that using MRI data, in general, the attachment sites of the ligaments in the knee can be determined with a reasonable accuracy. For some structures, however, the determination of the attachment sites is more complex, probably due to a larger area of attachment and a less apparent distinction on the MRI images. The implications of the variations found in the current study depend on the particular ligament, as some structures have a more pronounced effect on the joint kinematics and mechanics than others.

Conflict of interest

Competing interests: None declared

Funding: Hendi H. Rachmat was financially supported by a scholarship from the Directorate General of Higher Education (DIKTI)-Indonesia.

Ethical approval: Not required

Acknowledgments

The authors would like to thank the observers, T.G. van Tienen, M.D., PhD., P.K. Tomaszewski, Ir., PhD., José Smolders, M.D., Loes Nicolaas, M.D., and Siska Nurohmah, M.D. for their participation. Finally we thank Willem van de Wijdeven and René van der Venne for their input and Akkie Rood for helping to prepare the cadaver.

References

1. Li, G., Gil, J., Kanamori, A., Woo, S.L.Y., 1999. A validated three-dimensional computational model of a human knee joint. Journal of Biomechanical Engineering 121: 657-662.
2. Peña, E., Calvo, B., Martínez, M.A., Doblaré, M., 2006. A three-dimensional finite element analysis of the combined behavior of ligaments and menisci in the healthy human knee joint. Journal of Biomechanics 39: 1686–1701.
3. Potočnik, B., Zazula, D., Cigale, B., Heric, D., Cibula, E., Tomažič, T., 2008. A patient-specific knee joint computer model using MRI data and 'in-vivo' compressive load from the optical force measuring system. Journal of Computing and Information Technology – CIT 16: 209-222.
4. Suggs, J., Wang, C., Li, G., 2003. The effect of graft stiffness on knee joint biomechanics after ACL reconstruction-a 3D computational simulation. Clinical Biomechanics 18: 35-43.
5. Rathnayaka, K., Momot, K.I., Noser, H., Volp, A., Schuetz, M. A., Sahama, T., Schmutz, B., 2012. Quantification of the accuracy of MRI generated 3D models of long bones compared to CT generated 3D models. Medical Engineering & Physics 34: 357-363.
6. Besl, P.J. and McKay, N.D., 1992. A method for registration of 3-D shapes. IEEE Transactions on pattern analysis and machine intelligence 14: 239-256.
7. Victor, J., Van Doninck, D., Labey, L., Innocenti, B., Parizel, P.M., Bellemans, J., 2009. How precise can bony landmarks be determined on a CT scan of the knee? The knee 16:358-365.
8. Liu, F., Yue, B., Gadikota, H.R., Kozanek, M., Liu, W., Gill, T.J., Rubash, H.E., Li, G., 2010. Morphology of the medial collateral ligament of the knee. Journal of Orthopaedic Surgery and Research 5: 69.
9. Oakes, D.A., Markolf, K.L., Mc Williams, J., Young, C.R., McAllister, D. R., 2003. The effect of femoral tunnel position on graft forces during inlay posterior cruciate ligament reconstruction. The American Journal of Sports Medicine Vol 31 No 5: 667- 672.
10. Bedi, A., Maak, T. Musahl, V., Citak, M., O'Loughlin, P. F., Choi, D., Pearle, A.D., 2010. Effect of tibial tunnel position on stability of the knee after anterior cruciate ligament reconstruction: Is the tibial tunnel position most important? The American Journal of Sports Medicine Volume: XX, No. X.
11. Howell, S.M., 1998. Principles for placing the tibial tunnel and avoiding roof impingement during reconstruction of a torn anterior cruciate ligament. Knee Surg. Sport Traumatol, Arthrosc 6 (Suppl 1): S49-S55.
12. Zavras, T.D., Race, A., Amis, A.A., 2005. The effect of femoral attachment location on anterior cruciate ligament reconstruction: graft tension patterns and restoration of normal anterior-posterior laxity patterns. Knee Surg. Sport Traumatol Arthrosc 13: 92-100.
13. Galloway, M.T., Grood, E.S., Mehalik, J.N., Levy, M., Saddler, S.C., Noyes, F.R., 1996. Posterior cruciate ligament: an in vitro study of femoral and tibial graft placement. The American Journal of Sports Medicine Vol. 24, No.4: 437- 445.

14. Petersen, W., Lenschow, S., Weimann, A., Strobel, M.J., Raschke, M.J., Zantop, T., 2006. Importance of femoral tunnel placement in double-bundle posterior cruciate ligament reconstruction: biomechanical analysis using a robotic/universal force-moment sensor testing system. The American Journal of Sports Medicine Vol. 34, No.3: 456-463.
15. Mannor, D.A., Shearn, J.T., Grood, E.S., Noyes, F.R., Levy, M.S., 2000. Two-bundle posterior cruciate ligament reconstruction: an in vitro analysis of graft placement and tension. The American Journal of Sports Medicine Vol. 28, No. 6: 833-845.
16. Shearn, J.T., Grood, E.S., Noyes, F.R., Levy, M.S., 2004. Two-bundle posterior cruciate ligament reconstruction: how bundle tension depends on femoral attachment. The Journal of Bone & Joint Surgery Vol. 86-A, No. 6: 1262-1270.
17. Burns, W.C., Draganich, L.F., Pyevic, M., Reider, B., 1995. The effect of femoral tunnel position and graft tensioning technique on posterior laxity of the posterior cruciate ligament-reconstructed knee. The American Journal of Sports Medicine Vol. 23, No. 4: 424-430.
18. Bartel, D. L., Marshall, J. L., Schieck, R. A., Wang, J. B., 1977. Surgical repositioning of the medial collateral ligament: an anatomical and mechanical analysis. The Journal of Bone and Joint Surgery 59-A, No. 1: 107-116.
19. Meister, B.R., Michael, S.P., Moyer, R.A., Kelly, J.D., Schneck, C.D., 2000. Anatomy and kinematics of the lateral collateral ligament of the knee. The American Journal of Sports Medicine Vol. 28, No. 6: 869-878.
20. Baldwin, M.A., Lengenderfer, J.E., Rullkoetter, P.J., Laz, P.J., 2010. Development of subject-specific and statistical shape models of the knee using an efficient segmentation and mesh-morphing approach. Computer Methods and Programs in Biomedicine 97: 232-240.
21. Swanson, M.S., Prescott, J.W., Best, T.M., Powell, K., Jackson, R.D., Haq, F., Gurcan, M.N., 2010. Semi-automated segmentation to assess the lateral meniscus in normal and osteoarthritic knees. Osteoarthritis and Cartilage 18: 344-353.
22. Bryan, R., Nair, P.B., Taylor, M., 2009. Use of a statistical model of the whole femur in a large scale, multi-model study of femoral neck fracture risk. Journal of Biomechanics 42: 2171-2176.
23. Bryan, R., Mohan, P.S., Hopkins, A., Galloway, F., Taylor, M., Nair, P. B., 2010. Statistical modeling of the whole human femur incorporating geometric and material properties. Medical Engineering & Physics 32: 57-65.
24. Fitzpatrick, C.K., Baldwin, M.A., Laz, P.J., Fitzpatrick, D.P., Lerner, A.L., Rullkoetter, P.J. , 2011. Development of a statistical shape model of the patellofemoral joint for investigating relationships between shape and function. Journal of Biomechanics 44: 2446-2452.
25. Galloway, F., Worsley, P., Stokes, M., Nair, P., Taylor, M., 2012. Development of a statistical model of knee kinetics for applications in pre-clinical testing. Journal of Biomechanics 45: 191-195.